PHYSICAL REVIEW B **95**, 014426 (2017)

Advances in quantitative Kerr microscopy

I. V. Soldatov
Institute for Metallic Materials, Leibniz Institute for Solid State and Materials Research (IFW) Dresden, Helmholtzstrasse 20, D-01069 Dresden, Germany
and Institute of Natural Sciences, Ural Federal University, 620000 Ekaterinburg, Russia

R. Schäfer
Institute for Metallic Materials, Leibniz Institute for Solid State and Materials Research (IFW) Dresden, Helmholtzstrasse 20, D-01069 Dresden, Germany
and Institute for Materials Science, TU Dresden, 01062 Dresden, Germany

(Received 27 September 2016; revised manuscript received 29 November 2016; published 24 January 2017)

An advanced wide-field Kerr microscopy approach to the vector imaging of magnetic domains is demonstrated. Utilizing the light from eight monochrome light emitting diodes, guided to the microscope by glass fibers, and being properly switched in synchronization with the camera exposure, domain images with orthogonal in-plane sensitivity are obtained simultaneously at real time. After calibrating the Kerr contrast under the same orthogonal sensitivity conditions, the magnetization vector field of complete magnetization cycles along the hysteresis loop can be calculated and plotted as a coded color or vector image. In the pulsed mode also parasitic, magnetic field-dependent Faraday rotations in the microscope optics are eliminated, thus increasing the accuracy of the measured magnetization angles to better than 5°. The method is applied to the investigation of the magnetization process in a patterned Permalloy film element. Furthermore it is shown that the effective magnetic anisotropy axes in a GaMnAs semiconducting film can be quantitatively measured by vectorial analysis of the domain structure.

DOI: 10.1103/PhysRevB.95.014426

I. INTRODUCTION

The *integral* magnetic vector behavior of ferro- or ferrimagnetic materials can be measured by a number of techniques. For instance, magnetization loops can be obtained by means of vibrating sample magnetometry (VSM) available in a very simple configuration [1] or in extended versions of "true" vector VSM setups [2,3]. Also transport measurements using the anisotropic magnetoresistance [4–6] or MOKE (magneto-optical Kerr Effect) magnetometry in the case of magnetic films [7,8] can be applied. Integral measurements, however, cannot be used to extract information on the magnetic microstructure, which provides the link between the basic physical and macroscopic properties of a magnetic material [9]. Domain analysis is therefore essential for the interpretation of magnetization loops and for obtaining a deeper understanding of numerous relevant physical phenomena spanning the range from "traditional" applications of magnetic materials to the rapidly evolving fields of spin electronics, spin caloritronics, and spin orbitronics. All this promotes an ongoing development of techniques for direct domain imaging with the ultimate goal of an experimental measurement of a magnetization vector field.

For vectorial domain observation, a variety of magnetic microscopies have been developed to date, including scanning electron microscopy with polarization analysis (SEMPA) [10–12], electron holography [13,14], differential phase contrast Lorentz transmission electron microscopy [15–17], and methods based on soft x-ray spectromicroscopy [18,19]. Although most of these techniques provide a high lateral resolution in the ten nanometer regime, they require rather long exposure times, special sample preparation, or "big" machines like synchrotrons, which can make domain image acquisitions rather sophisticated and elaborate.

As for magneto-optical Kerr microscopy, already in the late 1980s Rave *et al.* [20] had introduced a technique for the quantitative analysis of magnetic domains. It is based on the merging of two images of the domain structure of interest, obtained with complimentary Kerr sensitivities, and by comparing the Kerr contrast with calibration curves obtained under the same complimentary contrast conditions. For experimental reasons, this first approach was restricted to the analysis of static domain images on strictly in-plane magnetized surfaces; it suffered from a low accuracy in the determined magnetization angles of around 20° at best and required mechanical and time consuming adjustments of the microscope optics. Recently an advanced approach was introduced [21], which is based on dichromatic imaging and which extended the method of quantitative Kerr microscopy to the analysis of complete magnetization processes. The experiment is computer controlled and consequently more time efficient than the classical method. However, the accuracy is still as low as previously, and the simultaneous imaging of the domains with two wavelengths adds additional inaccuracies in the lateral resolution.

In this article we will first review the principle of quantitative Kerr microscopy based on the classical approach in Sec. II. In Sec. III we will then briefly address the dichromatic technique before introducing an advanced technical realization of vectorial domain imaging that avoids most drawbacks of the previous methods. Examples will finally be presented in Sec. IV. They include the magnetization reversal process in a Permalloy patterned film element to demonstrate the capability of our approach to the quantitative imaging of magnetization processes, and second the investigation of magnetic anisotropy in a magnetic semiconductor film for which we make use of the high sensitivity of our method. The exact orientation of the

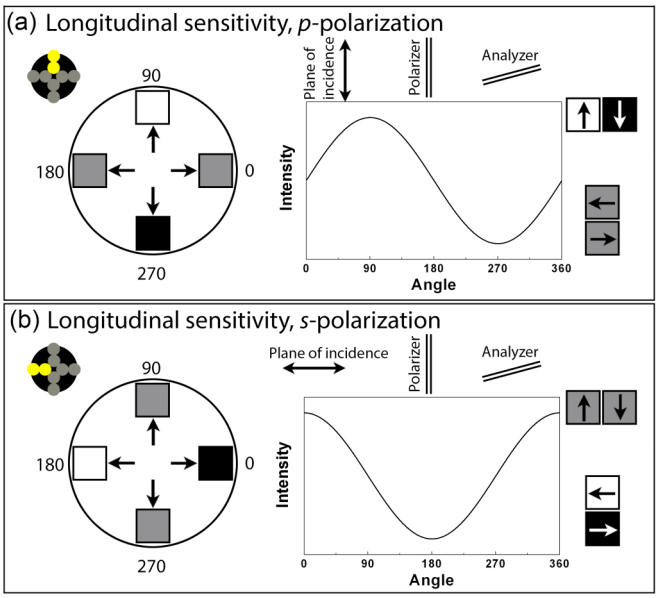

FIG. 1. Two phase-shifted complimentary sensitivity functions, required for quantitative Kerr microscopy, together with selected intensities for symmetric magnetization directions (schematically). From (a) to (b) the plane of light incidence was rotated by 90°, leaving the polarizer and analyzer unchanged. In our advanced approach this is realized by activating different LEDs in the diffraction plane as indicated by the insets showing the LED cross as seen in the conoscopic imaging mode of the microscope (showing the diffraction plane).

effective easy axes are extracted and compared with that found in electrical transport measurements [6].

II. CLASSICAL METHOD OF QUANTITATIVE KERR MICROSCOPY

According to Ref. [20], the reflected light intensity from an in-plane magnetized surface due to the Kerr effect depends on the orientation of the surface magnetization as

$$I = I_0 + Bm_l + Cm_t + D, \tag{1}$$

where m_l and m_t are the normalized longitudinal and transverse magnetization components (i.e., the components along and perpendicular to the plane of light incidence), I_0 is a combination of the squares of the normal (regularly reflected) light amplitudes N, the coefficients B and C are some combination of N and the Kerr amplitudes K, and D is an expression of the order of K^2 that is quadratic in the magnetization components. The normal contribution I_0 can be eliminated with the help of a difference image technique [22], and by opening analyzer and polarizer the N component becomes large so that the K^2 term can be neglected compared to the NK term. Finally, the intensity can be considered as a linear function of the magnetization components m_l and m_t.

For quantitative Kerr microscopy the independent coefficients B and C have to be determined experimentally and the Kerr intensity has to be calibrated. This requires two intensity measurements under complimentary sensitivity conditions as illustrated in Fig. 1: assume oblique light incidence along the vertical plane and p-polarized light [Fig. 1(a)]. Then opposite in-plane magnetizations at 90° and 270° result in a black and white contrast, whereas transverse magnetizations at 0° and 180° show up as intermediate gray. If plotted as a function of the magnetization direction, a sinusoidal-curve will result for the Kerr intensity. This calibration curve can, e.g., be measured by exposing the specimen to a magnetic saturation field that is rotated by 360° in steps. Now the intensity of a domain of interest can be compared with the calibration curve, and it turns out that there are two possible angles for the magnetization (with the exception of two extremum points). To come up with a unique angle, a second calibration curve is necessary that best is shifted by 90° to the first curve. In Fig. 1(b) this is realized by choosing a horizontal incidence plane with s-polarized light. If the intensity of our domain of interest under this second sensitivity condition is compared with the second calibration curve, ambiguities in the determination of the correct magnetization angle are resolved.

The common approach of quantitative Kerr microscopy thus requires the recording of two sinusoidal calibration functions with complimentary in-plane sensitivities that are phase shifted by 90°, providing two linear equations for the two magnetization components m_l and m_t, and the recording of two pictures of the domain structure of interest with unknown magnetization distribution under the two sensitivity conditions. In the first technical realization [20], the longitudinal and transverse Kerr effects with orthogonal in-plane sensitivity axes were utilized for the calibration functions. The Kerr sensitivity was adjusted by mechanically placing an aperture slit in the diffraction plane of the wide-field Kerr microscope at proper positions and by setting the analyzer and compensator accordingly (see Ref. [23] for a review of this "conventional" technique of wide-field Kerr microscopy). In a typical experiment the following procedure was applied: (i) setting of the first Kerr sensitivity, (ii) measurement of the first intensity calibration curve by saturating the sample in a rotating magnetic field, (iii) adjustment of the domain structure of interest by proper field history and recording of the domain pattern under the given sensitivity, (iv) leaving the domain state unchanged, but switching to the complementary Kerr sensitivity, (v) recording the domain pattern under the second sensitivity condition, and (vi) measurement of the second intensity calibration curve by saturating the sample in a rotating magnetic field.

This classical procedure suffers from numerous drawbacks: (i) As the domain pattern of interest is destroyed by measuring the second sensitivity curve, only *static* domain images can be analyzed quantitatively. (ii) Only domains with strict in-plane surface magnetization can be measured, owing to the calibration procedure that utilizes in-plane saturation. Furthermore, there is always a superposition of Kerr sensitivities to in-plane and out-of-plane magnetization components at the oblique incidence of light. Domains with out-of-plane surface magnetization components would thus reveal a polar Kerr contrast contribution that cannot be calibrated by in-plane fields [19]. (iii) Applied magnetic fields induce a Faraday rotation in the objective lens, which adds a field-dependent background intensity to the Kerr contrast. Furthermore, substantial stray fields may emerge from the magnetized sample itself in case of

bulk specimens, adding highly nonlinear Faraday contributions [24].[1] These parasitic Faraday contributions add to the Kerr intensity along the calibration curves, and they are in general different from those which are present when the domain pattern of interest is recorded, thus leading to errors in the contrast calibration and consequently to a decrease of the accuracy in determined magnetization directions—deviations from expected magnetization directions as high as 25° were reported [20]. By taking into account the Faraday contribution as a (assumed) linear function of the magnetic field, those deviations could be reduced down to typically 10° at best [25]. In some special cases the intensity calibration curves can be obtained by measuring the intensities of well-defined domains, without the necessity to apply fields for calibration [21,26,27]. Examples are iron silicon sheets or monocrystalline iron films, for which the magnetocrystalline anisotropy is strong enough to force the magnetization along the easy axes, or, e.g., patterned Permalloy ($Ni_{81}Fe_{19}$) films for which the calibration intensities can be taken from edge domains that are magnetized parallel to the edges for pole-avoidance reasons. However, the applicability of such a procedure is limited to the analysis of zero-field domain patterns as any field application would lead to the mentioned Faraday disturbances.

With the advanced approaches to quantitative Kerr microscopy, reported in the next section, most of these restrictions and drawbacks can be overcome.

III. ADVANCED APPROACHES TO QUANTITATIVE KERR MICROSCOPY

The employment of dual wavelength Kerr imaging, reported recently by von Hofe *et al.* [21], extends the method of quantitative Kerr microscopy to magnetization processes, thus overcoming the drawback of a restriction to static domain analysis mentioned in Sec. II. In their approach, the authors employ red and blue light-emitting diodes (LEDs), which are imaged to vertical and horizontal positions in the back focal plane of the microscope to achieve simultaneous Kerr sensitivities along the vertical and horizontal axes, respectively, on the sample. The two partial images can be separated by either using two cameras together with a dichroic mirror or by using a dichromatic image splitter between the microscope and camera. In both cases the two complementary domain images with orthogonal sensitivities, required for quantitative Kerr microscopy, and the two phase-shifted calibration curves are obtained *simultaneously* and not sequentially as in all previous approaches. Therefore a sequence of domain states along a magnetization curve can be quantitatively analyzed, which is a significant progress.

There are, nevertheless, a number of restrictions in that dichromatic approach: (i) A precise lateral matching of the images with complimentary sensitivities is required to prevent the appearance of artifacts in the resulting vector images. Especially for the solution with two cameras this is a challenging task. (ii) If the image splitter is used, the two partial images are displayed in the same camera frame, thus cutting the observable image area in half. (iii) By quantitatively combining two domain images that are recorded at two different wavelengths, imprecisions in the derived vector fields may arise especially for finely modulated magnetization configurations like domain walls. The differences in resolution can be up to 20% by using blue and red light in the dichromatic mode. (iv) Perfectly adapted dichromatic lenses and exact adjustment of the fiber ends along the optical axis are required in the microscope optics to avoid wavelength-dependent focus depths. (v) Finally, the parasitic Faraday contributions to the measured Kerr intensities, mentioned in Sec. II, are still present as soon as applied magnetic fields are involved.

All the restrictions and drawbacks of the before mentioned techniques for quantitative Kerr microscopy are resolved by an experimental approach which we propose in this paper. Here we make use of a LED light source that we have recently introduced in Ref. [28]. It consists of eight white LEDs (alternatively also monochromatic LEDs of the same color can be used), which are independently guided to the microscope by glass fibers. The fiber ends are arranged in a crosslike manner and they are imaged to the diffraction plane of the microscope (see Fig. 1, insets). Such an arrangement allows one to set the incidence direction just by turning

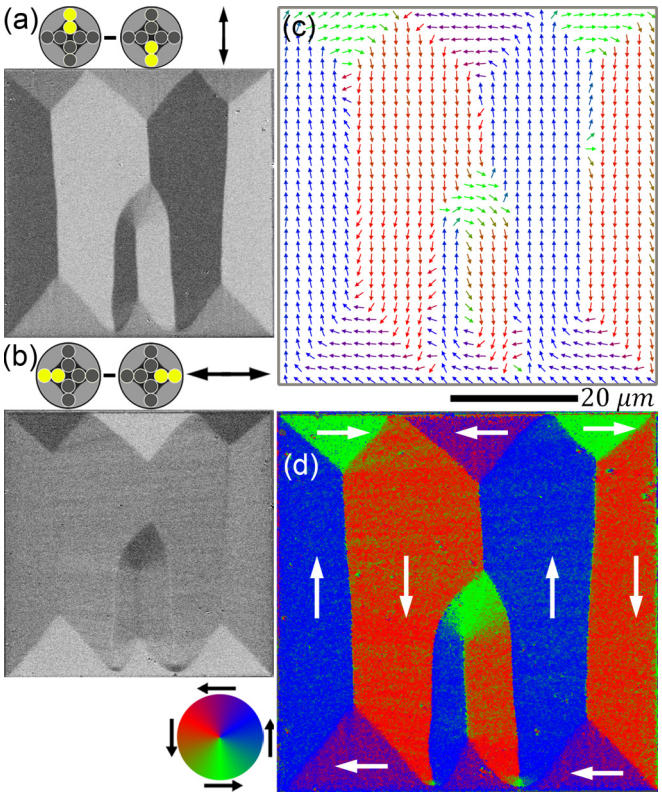

FIG. 2. Images of a zero-field domain state in a 240-nm thick Permalloy film element, obtained simultaneously at (a) vertical and (b) horizontal pure in-plane Kerr sensitivities by activating proper LEDs as schematically indicated in the insets. The (c) vector- and (d) color-coded plots of the magnetization vector field were quantitatively measured.

[1]The Faraday contributions, emerging from magnetized bulk specimens, were thoroughly analyzed in [24]. In that paper we have overlooked that this effect was already mentioned in [25] some 25 years ago.

ON and OFF the appropriate LEDs via computer control without any mechanical action. Driving the LED array in a pulsed mode with a typical switching time in the microseconds range in synchronization with the camera furthermore makes multicomponent imaging possible: Domain patterns can be imaged under orthogonal sensitivity conditions, e.g., longitudinal p-polarization (longitudinal vertical) and longitudinal s-polarization (horizontal) by alternately activating complementary LEDs on the vertical respective horizontal branches of the cross array as illustrated in Fig. 1. These two complimentary images are simultaneously displayed on the screen, thus providing the basis for quantitative Kerr imaging. For the term "simultaneously" it needs to be considered that the two complimentary images are obtained sequentially—unless the domain state does change noticeably within the exposure time (being of the order of some tenths of milliseconds), they may be considered as *simultaneously* acquired. Moreover, by subtracting the two images taken at opposite light incidence, pure in-plane Kerr sensitivity is achieved. In the latter mode also parasitic Faraday contributions are eliminated as was shown in Ref. [24]. For details on this advanced light source and the contrast separation, we refer to Ref. [28].

The advantages of this approach for quantitative Kerr microscopy are manifold: (i) Like in the dichromatic method, the required complimentary Kerr images are obtained simultaneously at real time without any mechanical action, thus allowing for the quantitative analysis of complete *magnetization processes*. As the complimentary images are recorded with the same camera, the mentioned alignment in case of the two-camera dichromatic solution is not required, and, compared to the image splitter version, full-frame images are displayed. (ii) As the same color of light is used for the complimentary images, the resolution and focus problems are not an issue. (iii) By running the LEDs in the pure in-plane mode, parasitic Faraday contributions are eliminated. This increases the accuracy of the quantitative vector analysis independent of applied magnetic fields. It furthermore abandons the restriction of the quantitative analysis to pure in-plane magnetized surfaces—now also pure, the in-plane component of *canted* magnetization vectors can be quantified, opening the path to a quantification of all three components of the magnetization vector. This extension is based on the fact that the length of the magnetization vector $\vec{m}$ is assumed to be 1 within the frame of micromagnetism, i.e., $|\vec{m}| = \sqrt{m_x^2 + m_y^2 + m_z^2} = 1$, leading to $m_z = \sqrt{1 - m_x^2 - m_y^2}$. If m_x and m_y are determined experimentally, the polar component can thus be calculated and plotted. For such analysis it is important that any deviations

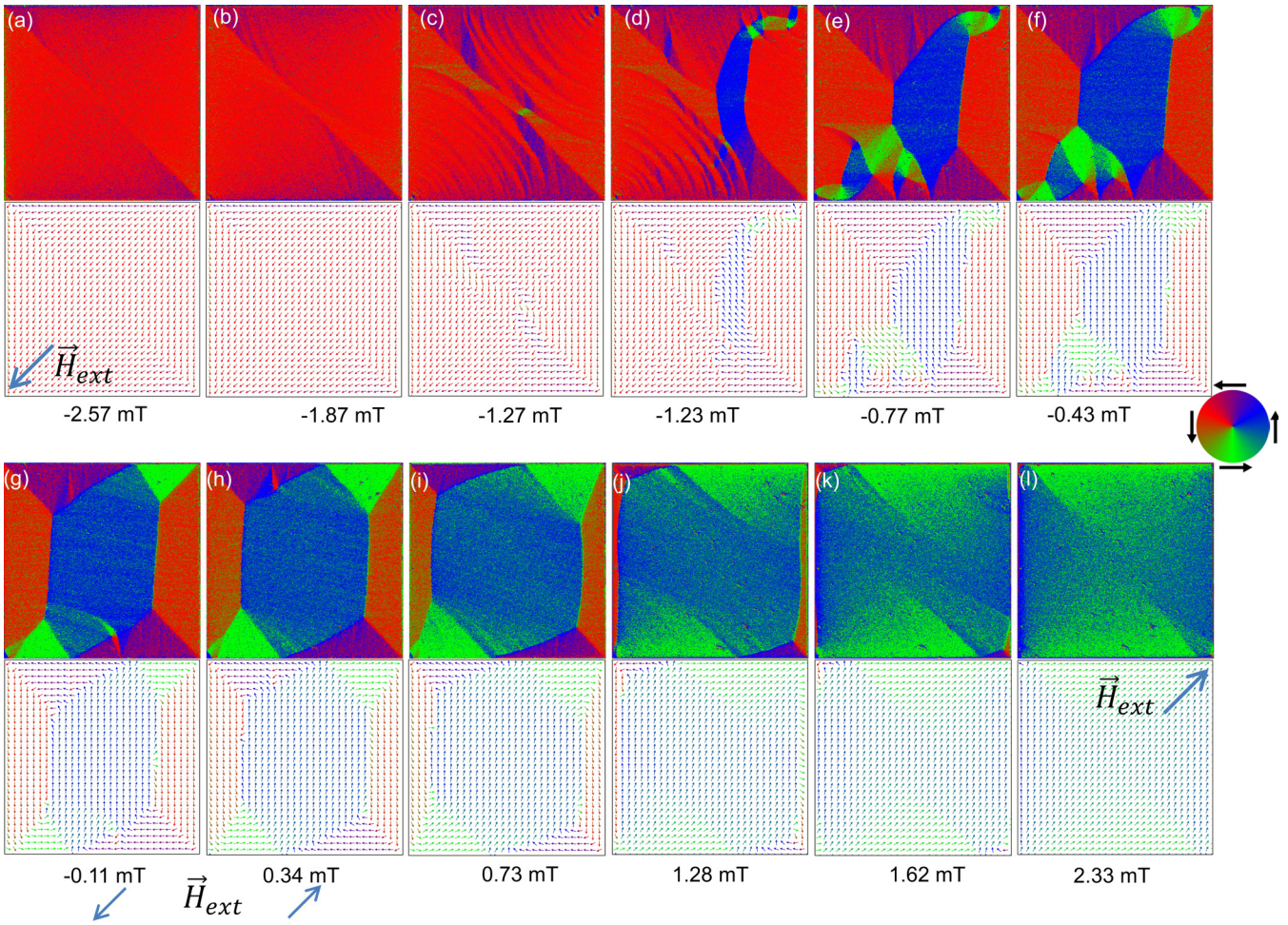

FIG. 3. The magnetization reversal process in the same Permalloy square element as in Fig. 2 in an external magnetic field along the diagonal axis. To see the details of the vector plots, we ask the reader to use an electronic version of this article and zoom into the plots.

of $m_x^2 + m_y^2$ from 1 due to noise, drift, or other inaccuracies are carefully avoided. If desired, the information on the out-of-plane component of magnetization can be also proceeded, by taking an additional image in a sequence with appropriate for pure polar sensitivity LEDs on [28].

IV. RESULTS

To demonstrate the viability of the method, it was first applied to the quantitative analysis of the domains in a patterned Permalloy element of a size in the ten micrometer range. For such big elements the domains and the magnetization process are well known [9] so that the obtained vector fields can be checked by plausibility arguments. The film has a thickness of 240 nm and an induced easy anisotropy along the vertical axis leading to a so-called Landau domain state at zero field with 180° basic domain walls and closure domains at the horizontal edges as shown in Fig. 2. The two pictures in (a) and (b) were imaged simultaneously at complimentary Kerr sensitivities along the vertical and horizontal axes, respectively, by pulsing the proper LEDs as indicated in the insets of the figure. Shown are zero-field difference images, which were obtained by subtracting a domain-free, gray-level background image that was achieved by applying an ac magnetic field along the diagonal axis and by averaging 16 frames. The two calibration functions (not shown) were measured by applying an external in-plane magnetic field of 20 mT magnitude that was rotated in steps of 30°. To avoid the effects of local inhomogeneities in the image intensity (caused, e.g., by a possibly inhomogenious illumination), the calibration functions were measured and calculated for each pixel individually. Then the orientation of the magnetization in each point (pixel) was determined by comparing the intensity of each two pixels of the original images (at orthogonal sensitivities) with the local calibration functions. The result of the quantitative analysis is presented in Figs. 2(c) and 2(d). The method works out well: The deviations of the calculated magnetization directions from expected ones are less than 5°, even for a Permalloy film with a rather low Kerr response.

As both complimentary domain images and the two corresponding calibration curves are obtained simultaneously, the presented technique can be applied to the imaging of dynamic processes. In Fig. 3 a sequence of quantitatively analyzed domain states at varying magnetic fields along the diagonal of the square is presented. Starting with an almost saturated state, the field was decreased in steps, resulting in the continuous formation of a concertina pattern that decays successively into a disturbed Landau state at zero field. With increasing positive field, rotational processes set in towards positive saturation. The observed behavior strongly supports theoretical calculations and experimental observations by means of conventional Kerr microscopy in Permalloy upon the diagonal magnetic field as reported in Refs. [29–31]. The sequence of images demonstrates the applicability of our technique to the quantitative imaging of dynamic domain processes.

Essentially, quantitative domain analysis can be used to determine the direction(s) of magnetic anisotropy, which directly influences the exhibited magnetic domain distribution and plays an important role in the way a magnetic media does respond to external stimuli. The result of such analysis

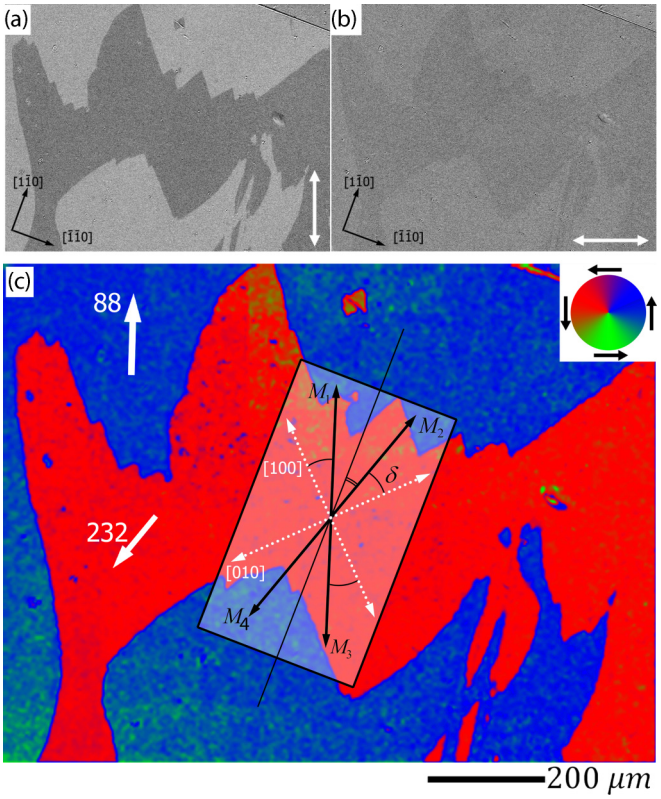

FIG. 4. Domain images of a GaMnAs film, taken by Kerr microscopy at zero magnetic field after ac demagnetization. Image (a) is obtained with sensitivity along the vertical axis and image (b) with sensitivity along the horizontal axis as indicated by white arrows. (c) Quantitative color plot of the domain structure. The white arrows represent the direction of the magnetization in the sample. Inset: schematics of the magnetic anisotropy at 20 K.

is presented next: A thin (200 nm) film of diluted magnetic semiconductor $Ga_{0.96}M_{0.04}nAs$ was shown [6] to have four effective easy axes (M_{1-4}), which exhibit temperature dependent orientations, being at a small angle δ to the [100], [010] crystallographic directions at low temperatures and approaching the [1$\bar{1}$0] direction with increasing temperature [see schematics in Fig. 4(c)].

Two images of the domain structure of interest were taken: one with the vertical [Fig. 4(a)] and the other with the horizontal Kerr sensitivity [Fig. 4(b)]. The line in the upper right corner of the images is the platinum stripe, used for positioning the sample with respect to the crystal axes and sensitivity directions. The left image has a much stronger contrast than the right one, indicating that the magnetization directions of the domains are pointing mostly in the vertical direction at a small angle to the [1$\bar{1}$0] direction. Figure 4(c) shows the quantitative evaluation of the domain structure after combining of two images with orthogonal sensitivities. The calculated distribution of the magnetization directions, with the exception of the topographical defects on the surface, reveals the occurrence of two domains with almost opposite directions of magnetization.

As the orientation of the platinum stripe (right upper corner), deposited on the surface of the sample for transport measurement (see Ref. [6]), in respect to crystallographic

axes is known, it can be seen that the sample in Fig. 4 is rotated clockwise so that the $[1\bar{1}0]$ direction is at 21° to the vertical image axis (see schematic). The deviation angle δ of the $M_{1,2,3,4}$ directions from the crystallographic [100], $[\bar{1}00]$, [010], and $[0\bar{1}0]$ directions can be easily calculated. For the red domain the angle between the experimentally determined M_1 and [010] directions is 26° and for the blue domain the angle between M_4 and [100] is 28°. The average angle $\bar{\delta} = 27° \pm 2°$ corresponds to a ratio between cubic and uniaxial anisotropy $K_u/K_{cub} = 0.8$, which is in agreement with the angle that was obtained by transport measurements [6] at a corresponding temperature of 20 K. Thus, this method provides an excellent accuracy, comparable with that of transport measurements, in spite the fact that $Ga_{0.96}M_{0.04}nAs$ being the most popular representative of diluted magnetic semiconductors demonstrates a very weak Kerr effect.

V. CONCLUSION

An advanced approach for the quantitative vectorial Kerr analysis was demonstrated. By recording two images with orthogonal sensitivities simultaneously and by merging them with the corresponding sensitivity calibration functions, the method can conveniently be applied to the quantitative imaging of the magnetization vector fields of complete magnetization processes. As parasitic Faraday contributions in the microscope optics are compensated and by using monochrome light, the accuracy and signal-to-noise ratio of the analysis is significantly enhanced compared to previous approaches.

The potential of the technique was demonstrated by the quantitative analysis of a remagnetization cycle of a Permalloy film element, and by the vectorial analysis of a domain structure in a GaMnAs thin semiconducting film with extremely low Kerr response. Here the effective magnetic anisotropy axes were determined and they were found to be in good agreement with those found in transport experiments.

The method can be easily extended for time-resolved imaging and to the analysis of surfaces with canted magnetization directions (not shown yet). Our approach to quantitative Kerr microscopy thus exceeds previous limits of the experimental instrumentation for magneto-optical investigation.

[1] T. El-Alaily, M. El-Nimr, S. Saafan, M. Kamel, T. Meaz, and S. Assar, J. Magn. Magn. Mater. **386**, 25 (2015).

[2] L. Jahn, R. Scholl, and D. Eckert, J. Magn. Magn. Mater. **101**, 389 (1991).

[3] P. Stamenov and J. M. D. Coey, J. Appl. Phys. **99**, 08D912 (2006).

[4] D. Shin, S. Chung, S. Lee, X. Liu, and J. Furdyna, IEEE Trans. Magn. **43**, 3025 (2007).

[5] D. Y. Shin, S. J. Chung, S. Lee, X. Liu, and J. K. Furdyna, Phys. Rev. Lett. **98**, 047201 (2007).

[6] I. V. Soldatov, N. Panarina, C. Hess, L. Schultz, and R. Schäfer, Phys. Rev. B **90**, 104423 (2014).

[7] P. Keatley, V. Kruglyak, R. Hicken, J. Childress, and J. Katine, J. Magn. Magn. Mater. **306**, 298 (2006).

[8] H. Ohldag, N. B. Weber, F. U. Hillebrecht, and E. Kisker, J. Appl. Phys. **91**, 2228 (2002).

[9] A. Hubert and R. Schäfer, *Magnetic Domains: the Analysis of Magnetic Microstructures*, (Springer, New York, 1998), p. 696.

[10] M. R. Scheinfein, J. Unguris, R. J. Celotta, and D. T. Pierce, Phys. Rev. Lett. **63**, 668 (1989).

[11] H. P. Oepen, G. Steierl, and J. Kirschner, J. Vac. Sci. Technol. B **20**, 2535 (2002).

[12] J. Unguris, M. R. Scheinfein, R. J. Celotta, and D. T. Pierce, Appl. Phys. Lett. **55**, 2553 (1989).

[13] A. Tonomura, J. Magn. Magn. Mater. **31-34**, 963 (1983).

[14] M. R. McCartney and Y. Zhu, J. Appl. Phys. **83**, 6414 (1998).

[15] A. C. Daykin, J. P. Jakubovics, and A. K. Petford-Long, J. Appl. Phys. **82**, 2447 (1997).

[16] J. Zweck, J. Chapman, S. McVitie, and H. Hoffmann, J. Magn. Magn. Mater. **104**, 315 (1992).

[17] M. C. Hickey, D.-T. Ngo, S. Lepadatu, D. Atkinson, D. McGrouther, S. McVitie, and C. H. Marrows, Appl. Phys. Lett. **97**, 202505 (2010).

[18] S.-K. Kim, J. B. Kortright, and S.-C. Shin, Appl. Phys. Lett. **78**, 2742 (2001).

[19] W. Kuch, R. Schäfer, P. Fischer, and F. Hillebrecht, *Magnetic Microscopy of Layered Structures* (Springer, New York, 2015), p. 246.

[20] W. Rave, R. Schäfer, and A. Hubert, J. Magn. Magn. Mater. **65**, 7 (1987).

[21] T. von Hofe, N. Onur Urs, B. Mozooni, T. Jansen, C. Kirchhof, D. E. Brgler, E. Quandt, and J. McCord, Appl. Phys. Lett. **103**, 142410 (2013).

[22] F. Schmidt, W. Rave, and A. Hubert, IEEE Trans. Magn. **21**, 1596 (1985).

[23] R. Schäfer, *Investigation of Domains and Dynamics of Domain Walls by the Magneto-Optical Kerr-Effect*, (John Wiley & Sons, Ltd, Hoboken, NJ, 2007).

[24] D. Marko, I. Soldatov, M. Tekielak, and R. Schäfer, J. Magn. Magn. Mater. **396**, 9 (2015).

[25] W. Rave and A. Hubert, IEEE Trans. Magn. **26**, 2813 (1990).

[26] W. Rave, P. Reichel, H. Brendel, M. Leicht, J. McCord, and A. Hubert, IEEE Trans. Magn. **29**, 2551 (1993).

[27] S. Defoug, R. Kaczmarek, and W. Rave, J. Appl. Phys. **79**, 6036 (1996).

[28] I. V. Soldatov and R. Schäfer, arXiv:1612.02027 (2016).

[29] R. Schäfer and A. Desimone, IEEE Trans. Magn. **38**, 2391 (2002).

[30] A. DeSimone, R. Kohn, S. Müller, F. Otto, and R. Schäfer, J. Magn. Magn. Mater. **242-245**, 1047 (2002).

[31] A. Barman, V. V. Kruglyak, R. J. Hicken, J. M. Rowe, A. Kundrotaite, J. Scott, and M. Rahman, Phys. Rev. B **69**, 174426 (2004).